Energy-dependent energy transfer: Deactivation of azulene (So, Evib) by 17 collider gases

ARTICLE *in* THE JOURNAL OF CHEMICAL PHYSICS · MAY 1983

Impact Factor: 2.95 · DOI: 10.1063/1.444669

3 AUTHORS, INCLUDING:

Michel J Rossi
Paul Scherrer Institut
261 PUBLICATIONS **6,403** CITATIONS
SEE PROFILE

John R. Barker
University of Michigan
170 PUBLICATIONS **5,857** CITATIONS
SEE PROFILE

Energy-dependent energy transfer: Deactivation of azulene (S_0, E_{vib}) by 17 collider gases[a)]

Michel J. Rossi, Jack R. Pladziewicz,[b)] and John R. Barker

Department of Chemical Kinetics, SRI International, Menlo Park, California 94025
(Received 8 November 1982; accepted 21 February 1983)

Collisional deactivation of highly vibrationally excited azulene in the electronic ground state was investigated using infrared fluorescence detection. Azulene (S_0, E) was prepared with $E \simeq 17\,500$ cm^{-1} and $E \simeq 30\,600$ cm^{-1} by laser excitation at 600 and 337 nm, respectively. Advantage was taken of the fast internal conversion rate to S_0 azulene from S_1(600 nm) and S_2(337 nm) electronic states. The collider gases investigated are He, Ne, Ar, Kr, Xe, H_2, D_2, N_2, CO, O_2, CO_2, H_2O, NH_3, CH_4, SF_6, n-C_4H_{10}, and unexcited azulene. The results are expressed in terms of $\langle \Delta E(E) \rangle$, the average energy transferred per collision, which can depend on the vibrational excitation energy E of the azulene. Using previously obtained knowledge of the dependence of infrared fluorescence intensity on E [M. J. Rossi and J. R. Barker, Chem. Phys. Lett. **85**, 21 (1982)], two methods were used to obtain $\langle \Delta E(E) \rangle$ values from the fluorescence decay curves: (1) an approximate method that considered only the average energy, and (2) solution of the full collisional master equation. Both methods gave $\langle \Delta E(E) \rangle$ values that depend strongly on E. The limited experimental information on the identity of the energy-transfer processes operative in the deactivation of azulene is discussed. Additional experimental results on vibration-to-vibration energy transfer from azulene to CO_2 are presented, which indicate that the emission at 4.3 μm observed previously [J. R. Barker, M. J. Rossi, and J. R. Pladziewicz, Chem. Phys. Lett. **90**, 99 (1982)] originates not only from CO_2(001), but from other states with one quantum of excitation in ν_3. The experimental results are discussed in terms of models for energy transfer, which have appeared in the literature. It is concluded that only a superficial understanding exists and theory has lagged far behind experiments on energy transfer.

INTRODUCTION

Intermolecular energy transfer involving highly vibrationally excited molecules in the electronic ground state is of crucial importance in pyrolysis, free radical combination, plasmas, discharge-pumped lasers, and laser-induced chemistry. Much information about energy transfer has been obtained from unimolecular reactions in the pressure fall-off regime, and from chemical and photoactivation experiments.[1,2] All of these experiments rely on a comparison between the specific decomposition rate constant $k(E)$, which depends on the vibrational energy of the molecule, and collisional deactivation. Most of these experiments involve more than one chemical reaction, necessitating a thorough and accurate assessment of the reaction mechanism and measurement of several different reaction products. This complexity can reduce the accuracy of the energy-transfer data and can reduce the sensitivity of the experiment to some details of the energy-transfer process. In addition, methods that rely on reactions with energy thresholds are not very sensitive to energy-transfer involving energies less than the threshold energy. Moreover, the accessible energy range using unimolecular reactions is usually very limited.

Recently, we reported preliminary results obtained using an experimental technique that does not rely on chemical reactions.[3,4] The technique employs infrared fluorescence from the excited molecules to monitor the rate of vibrational energy transfer from the excited molecules. Ensembles of nonreacting, highly vibrationally excited molecules are "prepared" by laser excitation. In the present paper, the unusual photophysical properties of azulene are exploited to prepare excited azulene and study its energy transfer. Infrared multiple photon absorption is a second promising method for preparing large concentrations of excited molecules.[5] In a recent publication, Wendelken *et al.*[6] described another direct method for investigating energy transfer. Their method is based on ultraviolet absorption that varies with excitation energy.

In the present paper, we report data on energy transfer involving excited azulene and seventeen different collision partners. The azulene was excited to initial vibrational energies of ~17 500 and ~30 600 cm^{-1}, and the results show that the average energy transferred from the excited azulene on every collision with unexcited collider gas depends on the vibrational energy of the azulene. In the following sections, the principles on which the experiments are based are explained, followed by a description of the experimental apparatus, a report of results, and discussion.

EXPERIMENTAL

Plan of experiments

In the present experiments, the rapid internal conversion processes of azulene[7] are exploited to prepare vibrationally excited azulene in the electronic ground state. A tunable dye laser and nitrogen laser are used to excite azulene to the S_1 and S_2 excited electronic states, respectively. Internal conversion to high vibrational levels of the electronic ground state takes place in 1.9 ps[8,9] and in ~2 ns[7] from the S_1 and S_2 states, re-

[a)]This work was supported by Contract CA-AM03-76SPO115 with the Department of Energy, Office of Basic Energy Science.
[b)]Summer faculty visitor, supported by the Industrial Research Participation Program of the National Science Foundation. Permanent address: Department of Chemistry, University of Wisconsin-Eau Claire, Eau Claire, Wisconsin 54701.

 0021-9606/83/116695-14$02.10

spectively, near the band origins; at energy levels above the band origin, internal conversion takes place more rapidly.[7] These internal conversion rates are much greater than collision frequency under the experimental conditions employed, and the result is an ensemble of vibrationally excited azulene molecules, which we assume to have an average energy equal to the sum of the photon energy and the initial thermal vibrational energy content of the azulene: $E = h\nu + E_t$. At 300 K (E_t = 979 cm^{-1}), the ensemble of excited molecules has a relatively narrow distribution of energies.

The particular advantages possessed by azulene are: (1) the excitation energies differ by about a factor of two; (2) the photophysics are "clean" and triplet-state formation is not important[10]; (3) the quantum yield of photoisomerization to give naphthalene is very low[11,12] and chemical reactions need not be considered; and (4) fluorescence quantum yields are also very low.[7] Although the S_1 and S_2 states can be selectively excited, the absorption coefficients are relatively low except over limited wavelength ranges. For this reason, experiments were carried out only at the two initial energies corresponding to 600 and 337.1 nm excitation wavelengths.

Azulene has 48 vibrational degrees of freedom, all of which are infrared active, and infrared fluorescence (IRF) from all of these bands can, in principle, be monitored.[13] The eight C–H stretching frequencies near 3000 cm^{-1} are well separated in wavelength from the other modes and can be detected with an InSb detector. The intensity of the IRF of each of the modes depends on the vibrational energy content of the molecule[14,15] and therefore the IRF intensity is used to monitor the internal energy of the excited azulene as it is collisionally deactivated,[3,4] as described below. Analysis of the rate of loss of internal energy for different collider gas pressures gives values for the average energy lost per collision.

APPARATUS

The experimental apparatus is shown schematically in Fig. 1. The fluorescence cell was 92 cm in length

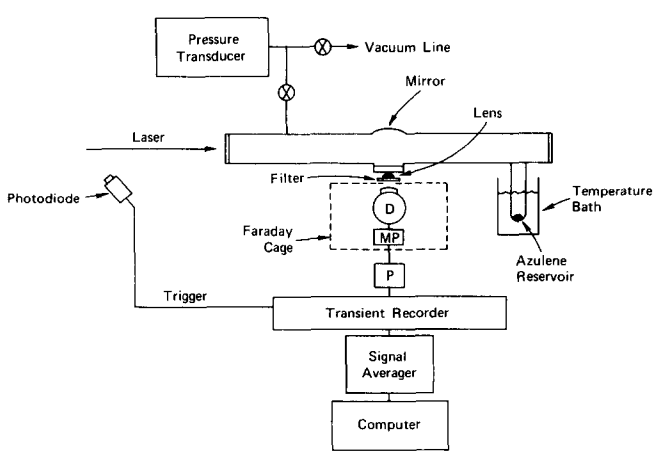

FIG. 1. Schematic diagram of experimental apparatus; D = Detector (InSb, 77 K); MP = Matched preamplifier; P = Preamplifier.

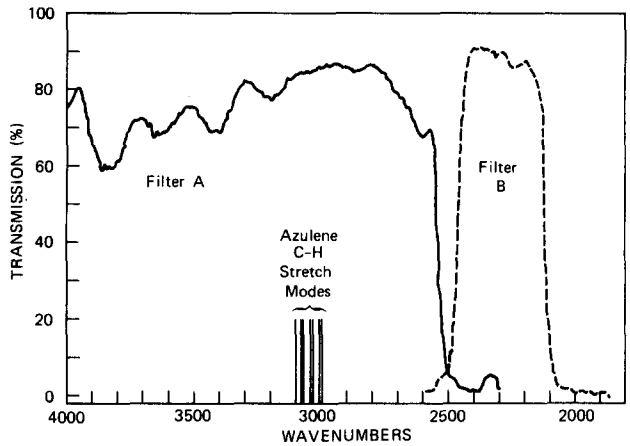

FIG. 2. IR filter transmission.

and 5 cm in diameter. The windows were sealed to the cell with viton *O* rings, which were lightly oiled with silicone diffusion pump oil. Quartz windows were used to admit the laser beam down the long axis of the cell; the long side arms reduced interference due to window fluorescence. The fluorescence was viewed through a KCl window by a 77 K InSb detector (Infrared Associates) equipped with a matched preamplifier. For many experiments, more fluorescence light was collected with a KRS-5 lens outside the cell and an Al-coated mirror opposite the window, as shown. The cell was connected to greaseless, mercury-free gas-handling system equipped with greaseless stopcocks fitted with viton *O*-rings, and it could be evacuated to $\lesssim 10^{-5}$ Torr. Leakage rates were $\lesssim 5$ m Torr/h. The azulene vapor pressure was regulated by cooling the azulene reservoir with a cryogenic cooler (Neslab).

Pressures were measured directly with calibrated electronic pressure transducers. During the course of this work, three different transducers were used: (1) Validyne model DP7; (2) Validyne model DP103, and (3) Baratron model 222HS-A-1. The first transducer was not designed for low pressures (< 100 m Torr), and we experienced difficulties with calibration and stability. The second transducer performed much better, although some difficulties were experienced with nonlinear response and calibration drift. The third transducer appears to be reliable for measurements reproducible to $\lesssim 0.5$ m Torr. Due to the various problems experienced with the pressure measurements, the results reported earlier[3,4,16] are not as reliable as those reported here. Due to these pressure measurement problems, many of the experiments were repeated to confirm the accuracy of the results.

The output of the infrared detector/preamplifier was amplified (Tektronix AM502) and captured with a transient recorder (Biomation 805); the digitized signal was summed by a signal averager (Nicolet 1070). The overall time resolution was ~1 μs and electronic filtering was sometimes used to improve the signal/noise ratio.

The IRF emission was isolated with bandpass interference filters. The spectra of the filters are shown in Fig. 2. For some experiments, a cold-gas filter (CGF)

was used, which was equipped with KCl windows and had an absorption pathlength of 2.1 cm.

The IRF temporal behavior was analyzed by two different methods during the course of this work. In the earlier experiments,[3,4] the nearly exponential decays were analyzed by digitally integrating the memory contents of the signal averager (to improve the S/N ratio) and taking the initial slope from the recorder traces of the integral. More recently,[16] the signal averager memory contents were transferred to a laboratory computer (Digital Equipment Corporation LSI 11/02) and analyzed numerically. Comparisons of the two methods showed random differences of ±15%, mostly due to the difficulties associated with reading the recorder traces.

The laser systems used in these experiments were: (1) a Chromatix CMX-4 tunable dye laser with 1–2 μs pulse length and ~1–3 mJ/pulse output energy; and (2) a nitrogen laser operating at 337.1 nm with 5–10 ns pulse length and 0.5–1 mJ/pulse energy.

The azulene used in the experiments was nominally 99% pure (Aldrich Chemical Company). For some experiments, the azulene was purified by vacuum sublimation, but no differences were noted between the purified and nonpurified azulene.

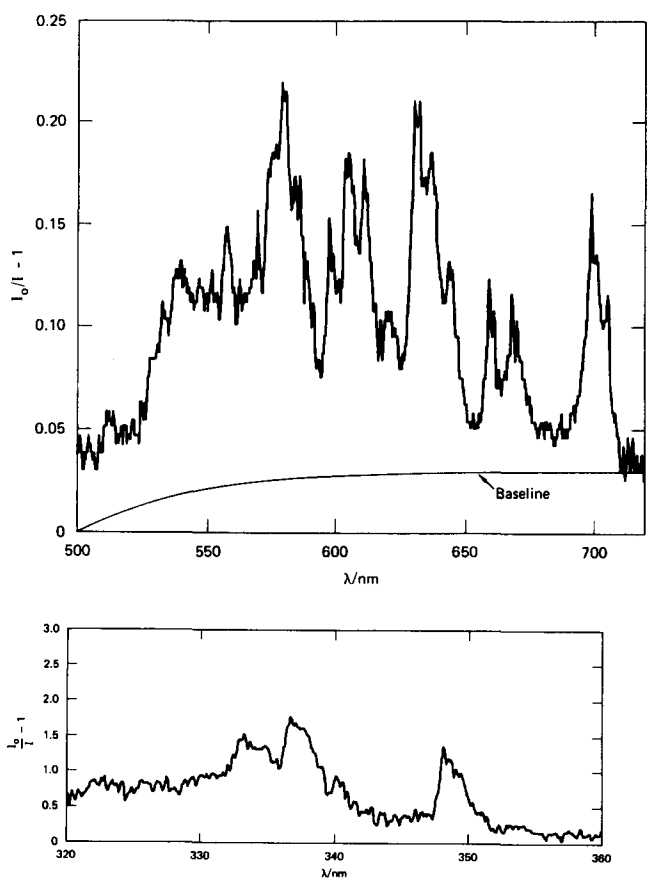

FIG. 3. (a) Azulene absorptinn spectrum. $S_1 \rightarrow S_0$ band (0.2 nm resolution). These spectra are representative examples for 10.9 mtorr azulene. For absolute absorption cross sections at four wavelengths, see Table I. (b) Azulene absorption spectrum. $S_2 \rightarrow S_0$ band (0.4 nm resolution). These spectra are representation examples for 10.9 mTorr azulene. For absolute absorption cross sections at four wavelengths, see Table I.

TABLE I. Azulene absorption coefficients.

λ (nm)	σ (cm^2)[a]	Estimated uncertainty
337	5.4×10^{-18}	±10%
537	4.2×10^{-19}	±20%
600	3.7×10^{-19}	±10%
670	2.7×10^{-19}	±10%

[a] $\sigma = (1/l[N])\ln(I_0/I)$.

Azulene absorption coefficient measurements

A single-beam absorption spectrophotometer was assembled from available components. The single-pass 3 m absorption cell was constructed from 25 mm diameter Pyrex tubing and fitted with greasless stopcocks and suprasil quartz windows. The cell was provided with an azulene reservoir, which could be isolated by a stopcock, and which was thermostated by means of a Neslab cryogenic cooler. The azulene vapor pressure in the cell was measured directly with a calibrated pressure transducer (Validyne, DP-103).

A 1000 W tungsten-halogen lamp (Oriel) was used as the light source and the image of the coil was focused on the entrance slit of the monochromator (McPherson model 227) by a 1 m focal length planoconvex quartz lens positioned between the lamp and the cell. For the visible (400–720 nm), the monochromator slits were set at 0.86 mm, corresponding to 0.4 nm resolution; in the near ultraviolet, the slit width was adjusted to maintain a constant resolution of 0.4 nm. In some of the absorption spectra, a 0.2 nm resolution has been used. The output signal from the red-sensitive photomultiplier (Hamamatsu R928) was stored by a digital oscilloscope/signal averager (PAR, model 4202) and recorded with an x-y recorder (Hewlett–Packard 4002B). The linearity of the photomultiplier tube response was established with seven neutral density filters, which were calibrated with a Cary 15 spectrophotometer.

The azulene absorption measurements were performed by scanning the lamp spectrum transmitted through the evacuated cell and storing the spectrum (I_0) in the signal averager memory. Azulene was then admitted to the cell and the pressure allowed to equilibrate for about one hour. A second spectrum (I) was recorded and the ratio I_0/I was displayed on the x-y recorder. The cell was then reevacuated and another spectrum (I_0') was recorded to compare with the first I_0 trace. Throughout this procedure, care was taken to minimize mechanical perturbations to the cell and monochromator, since this had a significant effect on the recorded spectrum. These measurements were repeated several times, and representative example spectra are shown in Fig. 3. Special attention was paid to the four wavelengths of exciting laser light that were used in the experiments, and the corresponding absorption coefficients are listed in Table I. The present results are not in quantitative agreement

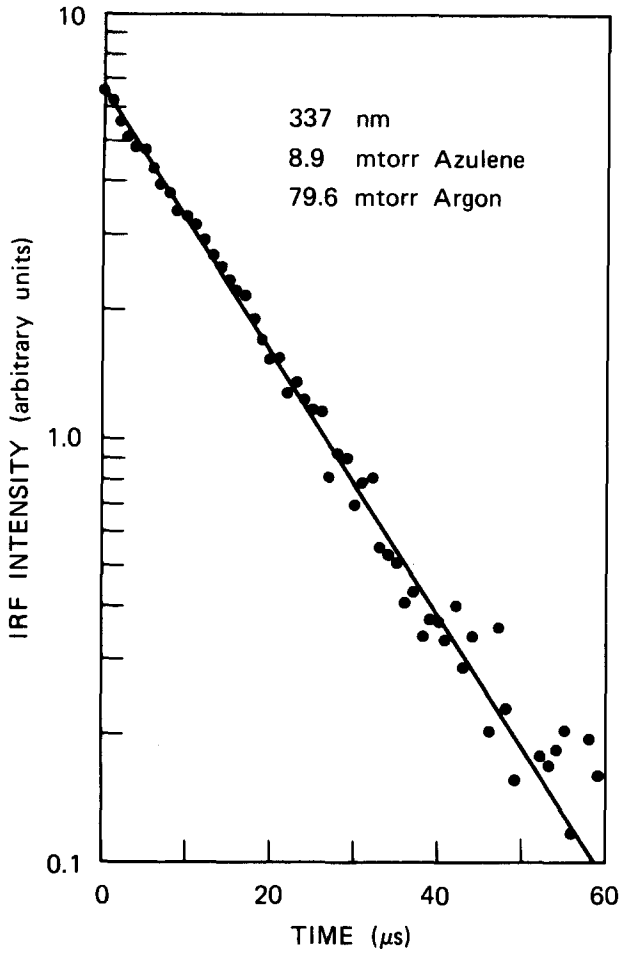

FIG. 4. Infrared fluorescence decay (filter A). Solid line is least-squares result for exponential decay (Table II).

with an earlier spectrum of gas-phase azulene reported in the literature.[11] The reason for the discrepancy is not known, unless it is due to the higher spectral resolution used in the present work.

The measured absorption coefficients, when combined with the laser powers and beam geometries of the experiments, indicate that less than 1% of the azulene is excited by either laser. Therefore, collision between two excited molecules can be neglected. The temperature rise in the irradiated gas can be estimated from heat capacities and the energy absorbed per pulse. The thermodynamic temperature rise is 30 K, calculated for a sample of pure azulene in which 1% of the azulene molecules is excited to an internal energy of 30 000 cm^{-1}. For azulene diluted by collider gases and for lower extents of excitation, the temperature rise in the experiments is reduced. Furthermore, in all mixtures, the temperature rise is reduced by thermal conductivity. Preliminary experiments[17] investigating the temperature dependence show that a 30 K temperature rise has a negligible effect on the results.

RESULTS

A typical IRF decay curve is shown in Fig. 4. Since the collisional deactivation of the excited azulene takes

TABLE II. Analysis of IRF decays (337 nm excitation).

Pressure (mTorr)		$I/I_0=\exp(-kt)$	$I/I_0=\exp(-kt+bt^2)$	
Az	Argon	10^{-4} k (s^{-1})	10^{-4} k (s^{-1})	10^{-8} b (s^{-1})
8.9	0	4.06 ± 0.02	3.94 ± 0.04	−0.72 ± 0.15
8.9	79.6	7.01 ± 0.05	6.44 ± 0.05	−2.78 ± 0.21
8.9	288.4	14.12 ± 0.15	14.12 ± 0.27	0.0 ± 2.8

place by a many-step cascade down the energy levels, there is no reason to expect that the IRF decay will be a simple exponential, as for a two-state system. The observed decays exhibit small deviations from pure exponential behavior,[3] but the deviations are very small, and the decays can be described in terms of phenomenological "rate constants." The Marquardt nonlinear least-squares algorithm[18] was used to obtain numerical fits to assumed forms for the decay curves. Examples of fits are presented in Table II for experiments chosen for their high precision. Inspection of the table shows that the deviations from simple exponential behavior are small and difficult to detect, considering the S/N of most of the experiments. Thus, for present purposes, the protocol adopted was to perform a least-squares fit to a simple exponential characterized by a phenomenological first-order rate constant.

The phenomenological first-order rate constants are observed to vary with the pressure of collider gas, as shown in Fig. 5. The variation observed mimics second-order kinetics in that a straight line is the result, permitting definition of the phenomenological second-order rate constant as the slope of the line. Thus, for each excitation laser wavelength, a single parameter—the second-order phenomenological rate constant—can be used to describe the temporal/pressure behavior of the IRF. At very low total pressures, however, this simple description breaks down, as illustrated in Fig. 5.[19] At pressures less than 2 mTorr, the mean-free-path of azulene is so large that the rate-limiting process

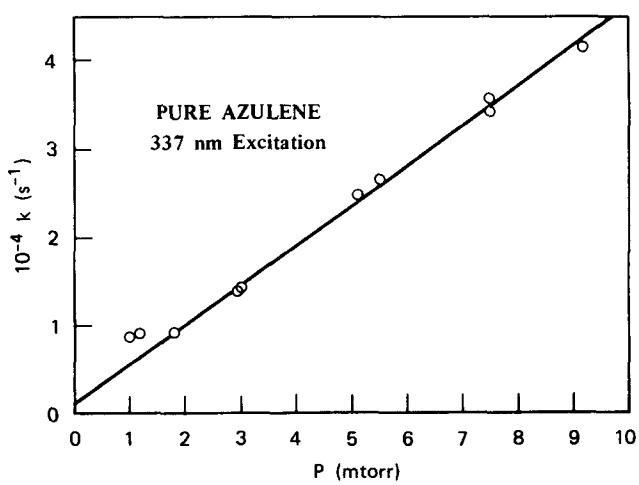

FIG. 5. Second-order kinetic plot, showing linear dependence of k on azulene concentration.

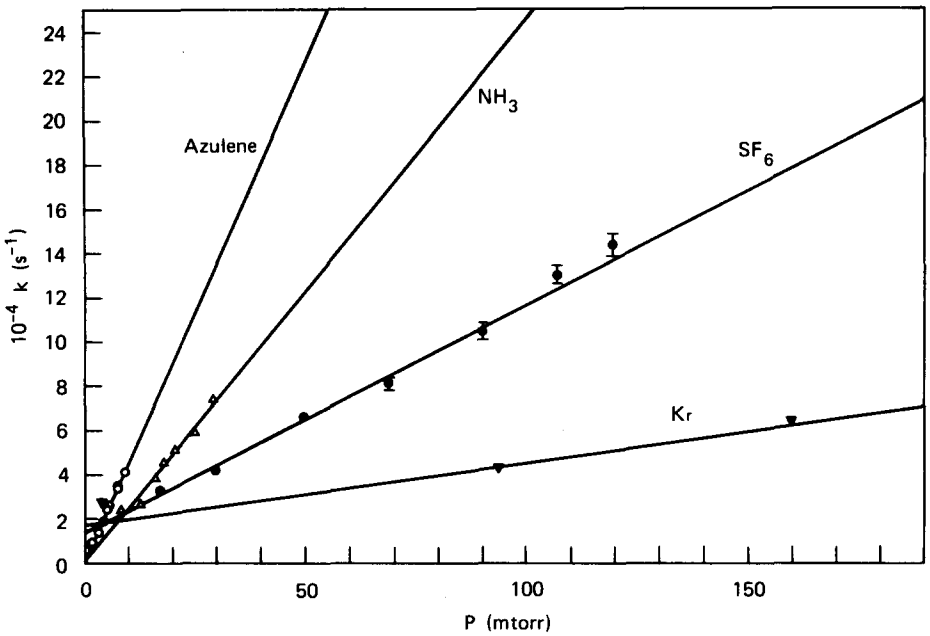

FIG. 6. Second-order kinetics plot for four collider gases (N_2 laser excitation).

is mass transport out of the field-of-view of the detector, resulting in the first-order rate constants becoming independent of pressure.

For each of seventeen collider gases, series of experiments were performed with excitation using the nitrogen laser and using the tunable dye laser. For excitation at 337 nm 4 000–20 000 laser shots were averaged; at 600 nm, 15 000–40 000 laser shots were averaged. For each collider gas and excitation wavelength, the procedure was to use a fixed pressure of azulene (2–5 mTorr, controlled by the thermostated reservoir temperature) and vary the pressure of collider gas. The resulting variation in dilution ratio did not complicate interpretation of the experiments because the decay rate of the IRF was found to be the sum[20] of that due to deactivation by azulene and deactivation by the collider gas: $\tau^{-1} = k_A[\mathrm{Az}] + k_M[M]$, where $[M]$ is the collider gas concentration. Thus, plots of τ^{-1} vs total pressure ($[\mathrm{Az}] + [M]$) gave straight lines with slopes equal to the phenomenological second-order rate constants k_M and intercepts equal to the quantity $(k_A - k_M) \times [\mathrm{Az}]$, where k_A is the azulene phenomenological rate constant. Several typical examples for nitrogen-laser excitation are presented in Fig. 6 and similar plots were obtained for dye-laser excitation. The phenomenological second-order rate constants were determined by weighted linear least-squares fits of the first-order rate constants (determined from "experimental" decays) vs pressure (for at least five different pressures). The resulting phenomenological second-order rate constants are presented in Table III.

TABLE III. Rate constants and collision parameters.

	Phenomenological rate constants[a]		Collision parameters		
Gas	10^{11} k(600 nm)	10^{11} k(337 nm)	σ (Å)	ϵ/k (K)	$10^{10} Z_{LJ}$
Azulene	25.2 ± 1.0	13.6 ± 0.3	7.68	590.0	12.44
He	0.663 ± 0.074	0.69 ± 0.09	2.551	10.22	10.87
Ne	0.794 ± 0.056	0.72 ± 0.12	2.820	32.8	6.37
Ar	1.29 ± 0.08	1.07 ± 0.03	3.542	93.3	6.49
Kr	1.25 ± 0.09	0.86 ± 0.04	3.655	178.9	5.80
Xe	0.974 ± 0.063	0.923 ± 0.060	4.047	231.0	5.70
H_2	4.71 ± 0.78	3.14 ± 0.16	4.827	59.7	29.40
D_2	2.75 ± 0.31	1.74 ± 0.09	4.827	59.7	20.95
N_2	1.48 ± 0.11	1.69 ± 0.30	3.798	71.4	7.47
O_2	1.56 ± 0.10	1.68 ± 0.10	3.467	106.7	7.16
CO	1.92 ± 0.09	2.20 ± 0.10	3.690	91.7	7.65
CO_2	3.54 ± 0.57	3.10 ± 0.10	3.941	195.2	7.72
H_2O	5.60 ± 0.59	6.92 ± 0.85	2.641	809.1	12.34
NH_3	5.09 ± 0.46	7.59 ± 0.52	2.90	558.3	12.02
CH_4	3.10 ± 0.13	3.70 ± 0.36	3.758	148.6	10.75
n-C_4H_{10}	11.7 ± 1.2	9.41 ± 0.28	4.687	531.4	9.94
SF_6	3.90 ± 0.30	3.14 ± 0.10	5.128	222.1	6.67

[a]Rate constants units of $cm^3\ s^{-1}$; uncertainties are ± 1 σ.

TABLE IV. Energy dependence of intensity.

Wavelength (nm)	Energy (cm^{-1})	Relative intensity	Equation (1)
670	15 904	0.12 ± 0.04	0.177
600	17 646	0.22 ± 0.09	0.225
537	19 601	0.26 ± 0.13	0.309
337	30 644	(1.0)	(1.0)

The objective of the present work is to determine the average amount of energy transferred per collision, based on the decay of infrared fluorescence. Two pieces of information are essential to carry out the analysis: collision rate constants Z and the dependence of infrared fluorescence intensity $I(E)$ on internal energy. With this information, a collisional master equation can be used to simulate the experiments and determine the energy transferred per collision $\langle \Delta E(E) \rangle$ as a function of vibrational energy residing in the molecule. A simpler analysis can also be performed which also gives good results.

Infrared fluorescence intensity [$I(E)$]

As discussed elsewhere,[4,15] $I(E)$ can be accurately approximated by:

$$I(E) = \sum_i \sum_{v_i=1}^{v_{max}} v_i A_i^{1,0} \frac{\rho_r(E - v_i h\nu_i)}{\rho(E)} , \quad (1)$$

where $A_i^{1,0}$ is the Einstein coefficient for spontaneous emission for the $0 \leftarrow 1$ transition of mode i, v_i is the quantum number of the mode, $\rho(E)$ is the total density of vibrational states (s modes), and $\rho_r(E - v_i h\nu_i)$ is the density of states of the $(s-1)$ vibrational modes, omitting the ith mode and the energy contained in it. This expression depends upon completely statistical distribution of energy within the molecule, as expected from our own experiments[3] and those of others,[22–24] and it is founded[14-15] on the harmonic oscillator approximation. This approximation is appropriate as long as v_i is small. For the eight C–H stretch modes of azulene, terms of the summation for $v_i > 1$ contribute only about 10%–20% for the highest energy of the present study.

To test the theoretical expression, we performed experiments at four excitation laser wavelengths and measured the initial IRF intensities relative to one another.[4] For these experiments, the two lasers were directed into opposite ends of the cell in a coaxial arrangement that maintained similar geometries for the two laser beams. Consecutive experiments were performed, holding azulene pressure, detector field-of-view and laser-beam geometries constant. Laser output energies were measured for both lasers with the same Scientech power meter, and azulene absorption coefficients at the four wavelengths were measured as described above. The initial IRF intensity $I_0(\lambda)$ was determined by back extrapolation of the observed decay curves to $t = 0$, because the first few microseconds of the decay were obscured by electronic pickup. The experimental results are summarized in Table IV.

In Table IV the energy was taken as the sum of the excitation laser photon energy and the thermal vibrational energy ($E_t = 979\ cm^{-1}$), calculated according to statistical mechanics and a vibrational assignment for azulene.[13] The observed relative intensities are reported, along with estimates of the uncertainties, based on a propagation of errors treatment. The large uncertainty associated with the datum for 537 nm is due to the low absorption coefficient, which results in few excited molecules and a low level of IRF. For comparison, the predictions according to Eq. (1) are also tabulated. A figure showing the functional form of Eq. (1) was published elsewhere.[4]

As reported earlier,[4] the agreement between the experimental data and the prediction according to Eq. (1) is very good, justifying its use in our theoretical analysis. It is appropriate to point out, however, that the simple theory employed neglects the interesting spectral shifts and broadenings that are of interest in other work. Some of these effects have been observed in the present experiments. For example, emission from pure azulene excited at 337 nm is nominally isolated with filter A, but about 20% of that emission intensity can also be observed with filter B (Fig. 2). This behavior may be indicative of emission from the "quasicontinuum" and may indicate that emission from the C–H modes of highly excited azulene broadens and shifts to the red. These effects do not influence the present results, but azulene may be a good subject molecule for spectroscopic studies of the quasicontinuum.

Collision frequencies

In order to derive $\langle \Delta E \rangle$ on a "per collision" basis, collision frequencies must be known. Azulene possesses a permanent dipole moment, and thus the Stockmayer potential is appropriate.[25,26] Due to the relatively large size of azulene, however, the collision frequency calculated according to the Stockmayer potential is within a few percent of that calculated according to the Lennard-Jones potential. Because the collision parameters for azulene are not well known, we decided to use the Lennard–Jones potential to describe the collisions. Moreover, this choice is convenient because Lennard–Jones collision integrals have been thoroughly studied and good approximate forms have been developed for them.[27,28]

The collision rate constant was calculated according to the standard formula[28]:

$$Z_{LJ} = N_0 \sigma_{12}^2 \Omega_{12}^{(2,2)} (8RT/\pi\mu_{12})^{1/2} , \quad (2)$$

where N_0 is Avogadro's number, μ_{12} is the reduced mass for particles number 1 and 2 (gram molar units), σ_{12} is the Lennard–Jones collision diameter, and $\Omega_{12}^{(2,2)}$ is the collision integral, given approximately by[28]:

$$\Omega_{12}^{(2,2)} = [0.636 + 0.567 \log(kT/\epsilon_{12})]^{-1} , \quad (3)$$

where ϵ_{12} is the Lennard–Jones well depth.

The Lennard–Jones parameters for dissimilar species were calculated from those of the pure substances according to the usual combining rules:

TABLE V. Energy transferred per collision.

Collider	$-\langle \Delta E(E) \rangle$ (cm^{-1})		$\alpha(E) = \beta + \gamma E$		
Gas	$\langle E \rangle = 17\,500$ cm^{-1}	$\langle E \rangle = 30\,600$ cm^{-1}	β	γ	Model
Azulene	1217 ± 48	1425 ± 31	750	0.013	*R*
He	37 ± 4	83 ± 11	0	0.0067	*E*
Ne	75 ± 5	147 ± 25	0	0.010	*E*
Ar	119 ± 8	215 ± 6	55	0.013	*E*
Kr	130 ± 9	193 ± 9	135	0.006	*E*
Xe	103 ± 7	211 ± 14	0	0.012	*E*
N_2	96 ± 16	139 ± 7	0	0.0085	*E*
D_2	79 ± 9	108 ± 6	30	0.007	*E*
N_2	119 ± 9	295 ± 52	0	0.014	*E*
O_2	131 ± 8	306 ± 18	0	0.0158	*E*
CO	151 ± 7	375 ± 17	0	0.0175	*E*
CO_2	276 ± 44	523 ± 17	145	0.016	*R*
H_2O	273 ± 29	730 ± 90	0	0.024	*R*
NH_3	255 ± 23	823 ± 56	0	0.023	*R*
CH_4	173 ± 7	448 ± 44	0	0.018	*R*
C_4H_{10}	707 ± 73	1234 ± 37	110	0.034	*R*
SF_6	351 ± 27	613 ± 20	190	0.015	*R*

$$\sigma_{12} = \tfrac{1}{2}(\sigma_{11} + \sigma_{22}) \ , \tag{4}$$

$$\epsilon_{12} = (\epsilon_{11}\epsilon_{22})^{1/2} \ . \tag{5}$$

The parameters for all pure gases except azulene were taken from Reid and Sherwood[29] and are based on gas viscosities; for convenience, the values are listed in Table III.

In our earlier work, the Lennard–Jones parameters were estimates based on estimates of azulene physical properties. The results were $\sigma = 7.68$ Å and $\epsilon/k = 590$ K. Better estimates[30] can be obtained by using actual vapor-pressure data[31] for liquid azulene to obtain the boiling point ($T_b = 544$ K) and using the "modified Lyderson method"[32] (with naphthalene as reference gas) to obtain the critical temperature ($T_c = 829$ K) and pressure ($P_c = 40.6$ atm). Lennard–Jones parameters may be derived from the usual formulas[33]:

$$\epsilon/k = 0.75\ T_c \ , \tag{6}$$

$$\sigma = \left(\frac{3}{2\pi}\ 17.28\ T_c/P_c\right)^{1/3} \ . \tag{7}$$

The resulting Lennard–Jones parameters are $\sigma = 6.54$ Å and $\epsilon/k = 622$ K. These "revised" parameters predict a collision rate constant Z at 300 K for pure azulene that is about 25% lower than the one listed in Table III, which is based on the "old" set of parameters. For collisions with O_2, the revised parameters predict the collision frequency at 300 K to be about 19% lower than the old parameters. Since the discrepancies are relatively small, the old parameters are retained in this paper for the purpose of calculating collision frequencies. For comparisons with other laboratories and other sets of parameters, it should be noted that the rate of energy change derived from our experiments is given approximately by:

$$\frac{d\langle E \rangle}{dt} = Z[M]\langle \Delta E \rangle \ ,$$

where $\langle E \rangle$ is the average internal energy and $\langle \Delta E \rangle$ is the average energy step. Thus, the *product* $Z\langle \Delta E \rangle$ is transferrable and independent of Lennard–Jones parameters.

Simple analysis for $\langle \Delta E(E) \rangle$

Before discussing the full collisional master equation calculations, considerable insight and information are provided by a very simple analysis. For energy steps that are small compared to vibrational energy E, we can write:

$$\frac{d\langle E \rangle}{dt} = Z[M]\langle \Delta E(E) \rangle \ . \tag{8}$$

The left-hand side of this equation can be approximated by

$$\frac{d\langle E \rangle}{dt} \approx \frac{dE}{dI(E)}\ \frac{dI(E)}{dt} \ .$$

The IRF decay curves are nearly exponential, characterized by decay rate $k[M]$; thus, we have:

$$\left(\frac{dE}{dI(E)}\right)_0 \{-I_0\, k[M]\} = Z[M]\langle \Delta E(E) \rangle \ , \tag{9}$$

where the rate constant is determined by the fluorescence decay. The result is:

$$\langle \Delta E(E) \rangle = -\frac{k}{Z}\, I_0 \left(\frac{dE}{dI}\right)_0 \ . \tag{10}$$

According to the expression for $I(E)$, for an initial excitation of 30 600 cm^{-1}, $I_0(dE/dI)_0 = 13\,030$ cm^{-1}; for an initial excitation of 17 500 cm^{-1}, $I_0(dE/dI)_0 = 6010$ cm^{-1}. The tabulated values of k and Z were used with these parameters to obtain the values of $\langle \Delta E(E) \rangle$ listed in Table V. The uncertainties tabulated with the $\langle \Delta E(E) \rangle$ values are based only on the uncertainties (1σ) associated with the phenomenological rate constants. The total uncertainties depend on the Lennard–Jones parameters and on errors due to our expression for $I(E)$, and these are difficult to estimate. For each *individual* gas, the *relative* errors in the two values for $\langle \Delta E(E) \rangle$ are probably

±20%. Inspection of Table V shows that $\langle \Delta E(E) \rangle$ is not constant, but shows a strong variation with internal energy for most of the gases investigated. Comparisons between different gases depend upon the accuracy of the Lennard-Jones parameters and must be done with caution. We estimate that the uncertainties in comparison among gases are probably less than ±30%. The relative ordering of $\langle \Delta E \rangle$ values in Table V is similar to those in recent literature tabulations,[1,2] indicating that relative errors in the present work may not be as large as ±30%.

The analysis just presented is approximate because the actual population does not cascade down the energy ladder without spreading; instead it spreads over a wide distribution as it descends. Because $I(E)$ is nonlinear, the spreading of the population about the mean results in an intensity variation. For this reason, we have used the complete collisional master equation to simulate the experimental data, but the approximate solutions described by Troe[34] might also have been used.

Collisional master equation calculations

The collisional deactivation of highly excited polyatomic molecules usually takes place in a stepwise fashion, resulting in a cascade mechanism. Collisional master equations that describe this process have been in use for many years to analyze the results of unimolecular reaction rate studies.[1,2] The details of implementation of the collisional master equation have been presented elsewhere,[35] but the main features will be briefly reviewed.

Consider a molecule with vibrational energy E immersed in a heat bath of collider gas. Every time the molecule experiences a collision, its internal energy may be decreased or increased, according to the collisional step-size distribution function $P(E, E')$, where E' is the vibrational energy after a collision. Since the form of $P(E, E')$ is not known, it is common practice to use arbitrary functional forms and then determine whether the model simulations are consistent with experiments. The collisional up transitions are related to down transitions by detailed balance. Thus, we need to assign a functional form $P_d(E, E')$ only for the down steps and use detailed balance to determine $P_u(E, E')$ for the up steps:

$$P_u(E, E') = \frac{\rho(E')}{\rho(E)} \exp(-(E' - E)/kT) P_d(E, E') , \quad E' > E , \tag{11}$$

where $\rho(E)$ is the vibrational density of states.

Several arbitrary functional forms have been proposed for $P_d(E, E')$, in which small steps or large steps are more probable. According to the "exponential" model, which is thought to be appropriate for inefficient colliders, small steps are more probable:

$$P_d^e(E, E') = \exp(-(E - E')/\alpha_e)/N_e(E) , \tag{12}$$

where α_e is a parameter related to the average step size and $N_e(E)$ is the normalization constant. For more efficient colliders, the "reverse exponential" model makes large steps more probable:

$$P_d^r(E, E') = \exp(3 + 2(E - E')/\alpha_r)/N_r(E) , \quad (E - \tfrac{3}{2}\alpha_r) \le E' < E , \tag{13}$$

where α_r is a parameter and $N_r(E)$ is the normalization constant. Both of these functions are quite arbitrary, but there is some evidence that the exponential model describes some types of energy-transfer processes.[2] For our purposes, the calculated IRF decay is found to depend on α_e or α_r, but it is substantially independent of the collision model chosen. This is advantageous, since the general conclusions will not depend on the collision model although the exact numerical values of α_e or α_r may differ. In our calculations, the exponential model was used when $\langle \Delta E(30\,600) \rangle$ is smaller than 400 cm^{-1} and the reverse exponential model was used for more effective colliders.

For either model, the parameter α may, in principle, depend on E. Because our data corresponds to only two initial values of E, we have allowed for a simple linear function:

$$\alpha = \beta + \gamma E , \quad \beta, \gamma > 0 . \tag{14}$$

For both models, one can define $\langle \Delta E \rangle$, the average energy transferred per collision:

$$\langle \Delta E(E) \rangle = \int_0^\infty P(E, E')(E' - E)\, dE' . \tag{15}$$

For values of E greater than the average thermal vibrational energy content E_t, $\langle \Delta E \rangle$ is negative; for $E < E_t$, $\langle \Delta E \rangle$ is greater than zero [Fig. 7(a)]. Calculated curves of $\langle \Delta E(E) \rangle$ for both models show similar, but not identical shapes; the difference is small and cannot be detected on the basis of our experiments. In other laboratories, experiments have been undertaken specifically to determine $P(E, E')$;[1,2,36] however, those experiments are not designed to determine the energy dependence of $\alpha(E)$, the objective of the present work.

Another commonly used measure of step size is the average energy transferred in a down step:

$$\langle \Delta E(E) \rangle_d = -\int_0^E P_d(E, E')(E' - E)\, dE' . \tag{16}$$

For the two models used, the integrals are closed forms [if it is assumed $N(E)$ = constant], and the results are:

$$\text{Exponential model:} \quad \langle \Delta E(E) \rangle_d^e = -\alpha_e(E) ,$$

$$\text{Reverse exponential model:} \quad \langle \Delta E(E) \rangle_d^r = -1.08\alpha_r(E) . \tag{17}$$

The master equation is solved by Monte Carlo techniques, as described in detail elsewhere.[35] Collisions of the excited molecules both with unexcited azulene and with the collider gas are explicitly included in the calculations so that dilution ratios corresponding to actual experiments can be considered. At each collision for a given trajectory, the IRF intensity according to Eq. (1) is recorded by a bookkeeping subroutine. After averaging over many trajectories, the calculated IRF decay is analyzed by the same nonlinear least-squares computer program[18] that was used to analyze the experimental data, and the rate constant determined. By trial and

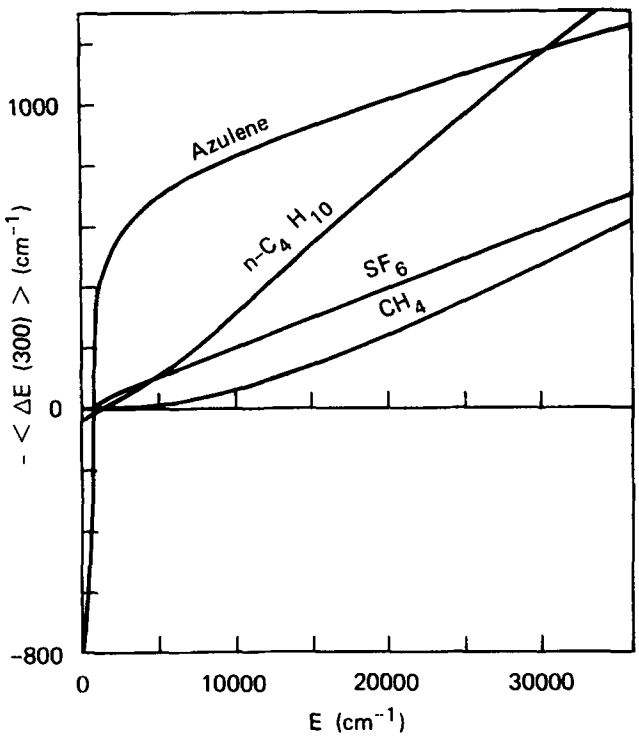

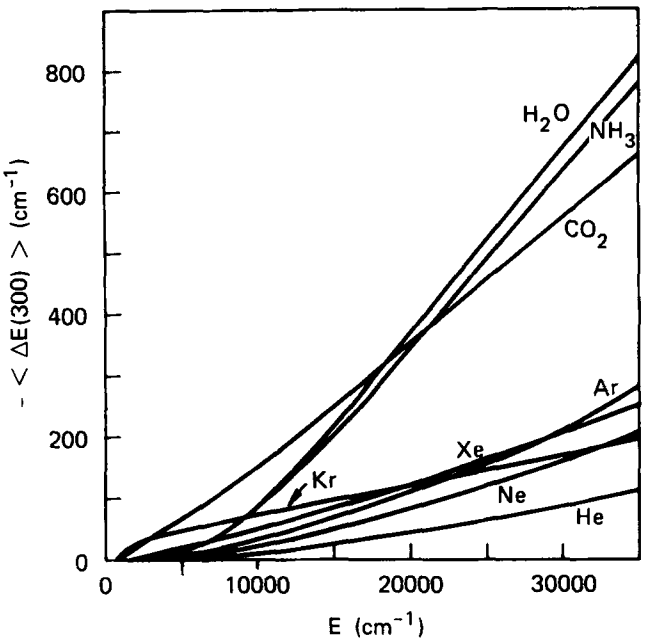

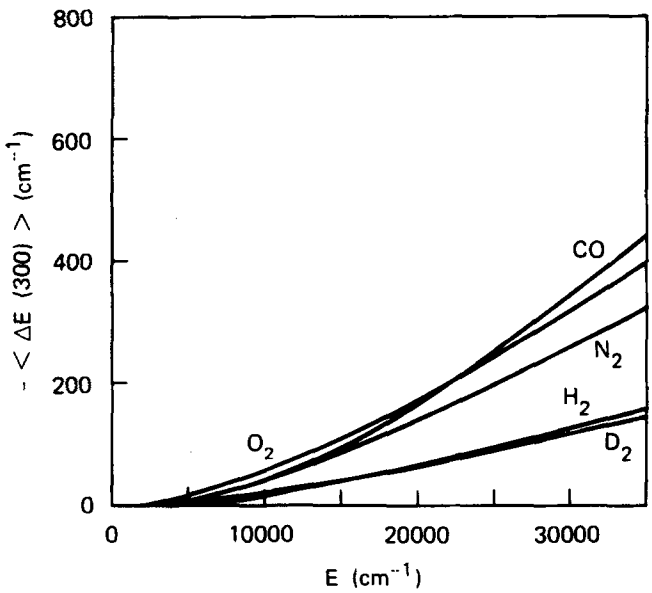

FIG. 7. Average energy transferred per collision. These curves for $\langle \Delta E(E) \rangle$ are based on $\alpha(E)$ from Table V; collisonal master equation fits to the experimental data of Table III. (a) Polyatomic gases; (b) rare gases and small polyatomic gases; (c) diatomic gases.

error, values of β and γ were selected to give $\alpha(E)$ functions and calculated rate constants consistent with the experimental data. Typically, the experimental data could be fitted within about $\pm 5\%$ although there were some exceptions, which indicated that the linear form assumed for $\alpha(E)$ is oversimplified.

The fitted values for β and γ for each collider gas are tabulated in Table V. Calculated values for $\langle \Delta E(E) \rangle$ for each gas based on $\alpha(E)$ are presented in Fig. 7. Generally, the values for $\langle \Delta E(E) \rangle$ presented in Fig. 7 compare well with those estimated according to Eq. (10), although there appears to be a slight systematic discrepancy for large step sizes, which are not as well approximated by Eq. (10).

It was pointed out earlier that the experimental decay curves are nearly, but not exactly, exponential decays. In fitting the calculated results to the experimental results, exponential decays were assumed. However, the calculated decay curves also showed nonexponential behavior similar to that exhibited by the experimental data. Examples of this behavior are presented in Table VI. Here, the values of $\alpha(25\,000)$ are identical, but γ and β are varied. Least-squares calculations were carried out assuming a simple exponential decay, or the more

TABLE VI. Computer simulations of IRF decays.[a]

$\alpha_r = \beta + \gamma E$		$I/I_0 = \exp(-kt)$	$I/I_0 = \exp(-kt + bt^2)$	
β[b]	γ[b]	$10^{-4}\,k$	$10^{-4}\,k$	$10^{-8}\,b$
0	0.043	4.19 ± 0.04	4.24 ± 0.07	0.36 ± 0.42
250	0.033	4.10 ± 0.05	3.98 ± 0.08	−0.64 ± 0.34
500	0.023	4.08 ± 0.06	3.74 ± 0.02	−1.64 ± 0.10
750	0.013	4.09 ± 0.07	3.48 ± 0.10	−2.62 ± 0.32
1075	0.0	4.10 ± 0.09	3.14 ± 0.08	−3.86 ± 0.27

[a]Conditions: 8.9 mTorr pure azulene, 337 nm excitation (see Table II for corresponding experimental results).
[b]Parameters chosen so that $\alpha_r(25\,000) = 1075\ \text{cm}^{-1}$.

complex form, as was done for the experimental data in Table II. The calculated decay curves show that single exponential decays are most closely approached when $\beta = 0$ and $\alpha(E)$ is directly proportional to internal energy.

The nonexponential behavior of the fluorescence decay is due to a combination of factors which include the multilevel cascade down the "ladder" of internal energy levels and, more important, the nonlinear dependence of $I(E)$ on internal energy. The effects of this latter factor can be understood in terms of Eq. (10), rewritten to read:

$$\frac{dI}{dt} = \left(\frac{dI}{dE}\right)\langle \Delta E \rangle Z[M]\,. \tag{18}$$

If $\langle \Delta E \rangle$ is a constant, the decay of intensity depends only on (dI/dE), if spreading of the population distribution is neglected. At high energies $(dI/dE)/I$ calculated according to Eq. (1) is greater than at low energies, and it is not constant, as required to produce an exponential decay of intensity. Between $E = 5000$ and 30 000 cm^{-1}, $(dI/dE)/I$ varies by nearly a factor of 20; low on the energy ladder, the value of $(dI/dE)/I$ is about 20 times greater than high on the ladder. Thus, the fluorescence tends to decay more rapidly at low energies, if $\langle \Delta E \rangle$ is the same on all parts of the energy ladder. If $\langle \Delta E(E) \rangle$ is energy dependent and smaller at low energies than high on the ladder, its influence tends to counteract the effects of the variation of $(dI/dE)/I$, causing the decay curves to behave more like simple exponentials.

The calculated results presented in Table VI also illustrate that the decay curves are not very sensitive to the form of $\langle \Delta E(E) \rangle$. Unless data of extremely high precision are obtained, the functional behavior of $\langle \Delta E(E) \rangle$ cannot be determined accurately from the shape of the fluorescence decay curve. If data corresponding only to one excitation laser wavelength are available, any reasonable functional form of $\langle \Delta E(E) \rangle$ can provide a reasonable fit to the data. Our conclusion that $\langle \Delta E(E) \rangle$ is energy dependent is the direct result of obtaining data for two different excitation wavelengths.

Experimental identification of the energy-transfer process

Recently, we reported[16] the results of experiments in which IRF from excited CO_2 was observed as a result of the process

$$CO_2(000) + Az(E) \rightarrow CO_2(nml) + Az(E')\,, \tag{19}$$

where Az represents azulene. The IRF from $CO_2(nml)$ was isolated with filter B (Fig. 2), and it was readily attenuated when CO_2 was admitted to the cold gas filter. By measuring the relative intensity of emission from CO_2 and from the azulene C–H modes, and correcting for filter transmission and detector response, we estimated that for N molecules of azulene initially excited by the nitrogen laser, about $(0.015 \pm 0.005) \times N$ molecules of CO_2 were excited to the (nml) state, after the azulene was fully deactivated. Because each initially excited azulene molecule possesses enough excitation energy to produce a dozen excited $CO_2(001)$ molecules, we concluded that V–V energy transfer from azulene to the asymmetric stretch mode of CO_2 was a relatively unimportant process.

We have carried out additional experiments using the cold gas filter. The attenuation of the CO_2 fluorescence due to CO_2 in the filter is presented in Fig. 8. These data were obtained by least-squares fitting of the observed IRF decay to the sum of two exponentials. One of the components is due to azulene fluorescence at 4.3 μm, and the other is due to CO_2 emission. The initial magnitude of the latter component is plotted in Fig. 8. Example data and further details are presented in Ref. 16. The calculation of Weitz and co-workers[37] predicts that for one Torr of CO_2 in the filter, virtually no emission will be observed, if the emitting state is solely $CO_2(001)$. In our experiments, however, about 40% of the emission is still transmitted by the filter. We conclude from this observation that the residual emission originates from difference bands $(nm1) - (nm0)$ where the identities of quantum numbers n and m are not yet known. It also seems likely that vibrational levels of CO_2 in addition to $(nm1)$ may be populated by the ener-

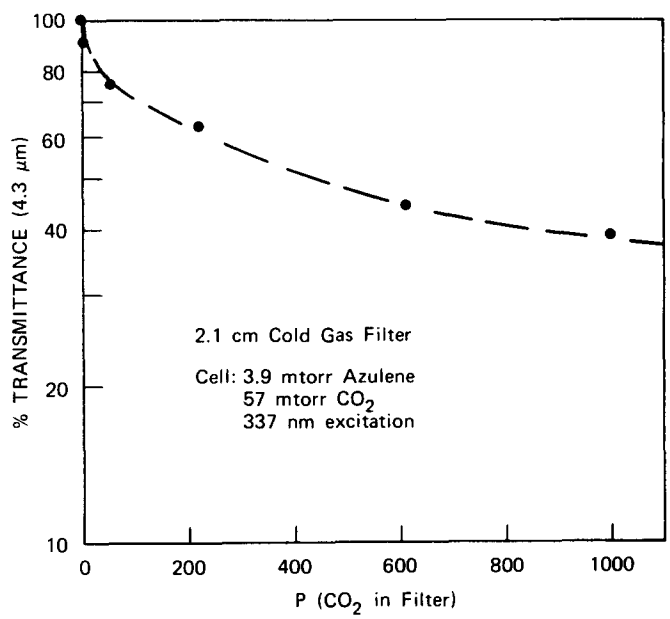

FIG. 8. Attenuation of 4.3 μm fluorescence (filter B) by cold gas filter. Pressure in mTorr.

gy-transfer process. Further experiments are desirable to investigate this possibility.

DISCUSSION

Inspection of Table V and Fig. 7 shows that all of the collider gases studied exhibit pronounced variations of $\langle \Delta E \rangle$ when the excitation energy is varied. This conclusion is independent of the two different sets of assumptions made in analyzing the data by the two methods and appears to be quite general. The relative ordering of $\langle \Delta E \rangle$ magnitudes seems similar to those derived from unimolecular reaction studies,[1,2] but the actual magnitudes reported here are at the lower end of the range of published values, as noted in the excellent direct studies of energy transfer by Troe and co-workers.[38] These workers feel that the unimolecular rate studies are subject to systematic errors if relative collision efficiencies are based on the assumption that the parent gas is completely effective in deactivating the excited molecule. If the collision efficiency of the parent gas is overestimated, $\langle \Delta E \rangle$ magnitudes of the other colliders will be overestimated. We feel that this explanation may apply in some cases, but the collision efficiency of the parent gas is not always assumed to be unity in the unimolecular rate studies, and it is possible that other explanations must be sought. In addition, azulene is a somewhat unusual molecule, and its behavior may not be representative of less rigid molecules which have free rotors.

Before dicussing the present results more fully, it is useful to consider approximate models for the energy-transfer process involving large polyatomics. For small small molecules at levels of excitation corresponding to only a few vibrational quanta, theories of energy transfer have been developed extensively and much insight into the energy-transfer process has been gained.[39] At low levels of excitation, V–V energy transfer often is the dominant mechanism and V–T/R energy transfer is rather slow in comparison.

At the upper end of the energy ladder, above the lowest threshold for unimolecular reactions, it is not known whether V–V or V–T/R energy transfer dominates. A "family" of theories of energy transfer has been developed to rationalize experimental data derived from unimolecular reaction rate studies, and common to these theories is the concept of a collision complex, which persists for a short time, τ. During the interval τ, energy can flow among the modes of the complex, subject to various assumed restrictions—the restrictions distinguish the theories. If no restrictions are introduced, the magnitude of $\langle \Delta E \rangle$ is grossly overestimated.[40–43] Most of the assumed restrictions refer to the flow of energy among the s vibrational modes of the excited molecule, and the t "transitional modes,"[41] which are associated with the relative coordinates of the two collision partners. For an excited polyatomic molecule colliding with bath gas M, $t = 3$ for atomic M, $t = 5$ for linear M, and $t = 6$ for nonlinear polyatomic M.

Schlag and co-workers[40,44] assumed that two restrictions limit the extent of energy transfer in the collision complex: (1) the finite duration of the collision, and (2) the internal modes of the collision partner play no role (i.e., V–T/R energy transfer, only). Energy is carried away by the transitional modes after the collision. If τ is long enough for perfect equilibration among the $s + t$ modes, the magnitude of $-\langle \Delta E \rangle$ is, again, overestimated, and it was concluded by Schlag and coworkers that the collision duration is too short to permit full redistribution of energy.

Lin and Rabinovitch[41] adopted the assumptions that energy can flow rapidly among the $s + t$ modes of the complex and that the internal modes of the collision partner are isolated. Rather than consider the duration of the collision, however, these workers introduced the idea that angular momentum conservation restricts the amount of energy that can be converted to relative motion. Using this "cutoff" of energy as an adjustable parameter, they obtained agreement with data for more than 100 collider gases. More recently, the question of angular momentum conservation was examined more quantitatively by Oref and Rabinovitch[45] and by Bhattacharjee and Forst,[43] and it was concluded that the restriction imposed by angular momentum conservation is not sufficient to account quantitatively for the small magnitude of $\langle \Delta E \rangle$. This model, like that of Schlag and co-workers, predicts on V–V energy transfer, at variance with our results.

Bhattacharjee and Forst[43] performed calculations to test the effects of finite collision duration and slow energy redistribution. Since the duration of a collision is finite and energy redistribution is not instantaneous, there is a dynamical restriction on the amount of energy that can be transferred to the transitional modes and to the internal modes of the collision partner. To implement the model, the authors first developed a method to estimate τ, the collision duration. They then assumed that the lifetime of the collision complex with respect to redissociation must equal τ. If all degrees of freedom are considered, unimolecular dissociation is predicted to be much too slow, and they concluded that, at most, only one oscillator of molecule M interacts effectively with the other degrees of freedom of the complex. The calculations are rather involved, but the results are in good agreement with experimental data.

Another approximate model intended to include the effects of finite collision duration is that of Schranz and Nordholm.[46] According to this model, all modes are involved, but the relative coordinates that correspond to bending and stretching motions are treated as square-well potential interactions, rather than harmonic oscillators. The idea here is that the collision event is of infinitesimal duration and thus the modes act like particles in a box. The predictions of the model are in fair to good agreement with experimental data.

It seems likely that a correct description of the energy-transfer process at high vibrational-state densities must include elements of all of these models, as well as other factors which may depend on "propensity rules." Propensity rules have been formulated for deactivation of small molecules with sparse densities of states.[39] Such rules may also be in effect at higher levels of excitation. Tang and Parmenter[47] have recently discussed state-to-state energy transfer involving benzene (S_1) for

vibrational energies ranging from zero to ~2500 cm^{-1}. Because the state density is low, they were able to distinguish details of the energy-transfer process which are obscured at higher state densities. On the basis of an assumed dependence of V–T/R energy transfer on reduced mass, they concluded that at low vibrational energies, V–V energy transfer dominates over V–T/R energy transfer, and the reverse is true at the upper end of the range investigated. If this conclusion is correct, it fits in nicely with results obtained for small molecules (low-state densities), as well as with the family of models of energy transfer at high-state densities. Further studies are needed to investigate this transitional behavior and to test for the effects of propensity rules on the energy-transfer process.

The theories described above were developed primarily to explain unimolecular reaction rate data and little attention was paid to the possible energy dependence of $\langle \Delta E(E) \rangle$, but all of the models explicitly predict that $\langle \Delta E \rangle$ is not constant. The simplest classical model assumes that a constant fraction of energy is apportioned between the collision partners, so that we have,

$$A(E) + M \rightarrow A(E') + M(E'')$$

$$\Delta E = (E' - E) = (1 - E''/E) \cdot E \ .$$

Classically, E''/E is a constant, independent of energy, and $\langle \Delta E \rangle$ is directly proportional to initial energy E.

A second simple example of the predicted energy dependence of $\langle \Delta E \rangle$ is provided by the unrestricted statistical model described above. This model predicts magnitudes of $\langle \Delta E \rangle$ that are too large, but the relative values for different collider gases are in rough agreement with experiment. Recently, Nordholm, Freasier, and Jolly (NFJ)[42] presented an approximate analytical form for this model, which is convenient for the present discussion. According to the NFJ analytical approximation,

$$-\langle \Delta E(E) \rangle = \frac{(n_2 + 2)}{(n_1 + n_2 + 4)} \left[E - E_t - \tfrac{3}{2} kT \right] ,$$

where n_1 and n_2 are molecular parameters, E_t is the thermal vibrational energy content of molecule A at temperature T, and E is the initial vibrational energy of the excited molecule. Parameters n_1 and n_2 depend on the number of vibrational modes s_i:

Type	n_1 (Excited molecule)	n_2 (Collider)
Atom	...	2
Diatomic or linear	$2\,s_1$	$2\,s_2 + 4$
Nonlinear	$2\,s_1 + 1$	$2\,s_2 + 5$

For azulene, $s_1 = 48$ and $n_1 = 97$. The NFJ expression predicts $\langle \Delta E(E) \rangle$ magnitudes that are much larger than those observed experimentally, but it predicts about the right ordering of magnitudes for various gases. Most important for this discussion, the model predicts a linear dependence for $\langle \Delta E(E) \rangle$, somewhat similar to the variation observed in Table V and Fig. 7, and it properly predicts $\langle \Delta E \rangle$ is greater than zero for energies less than E_t.

Although the simple classical model and the NFJ model are very crude and much refinement is necessary for quantitative predictions, both models illustrate that $\langle \Delta E(E) \rangle$ may exhibit a definite and predictable variation with initial energy. Although the effects of V–V and V–T/R energy transfer are superimposed for all 48 vibrational degrees of freedom in azulene, the result may be relatively simple, due to the extensive averaging involved. However, it does not follow that all colliders are expected to behave in the same way. Inspection of Fig. 7 and Table V shows considerable differences in behavior for different gases.

In experiments using time-resolved UV absorbance, Troe and co-workers[6,38] have directly observed energy transfer involving highly excited toluene (and substituted cycloheptatrienes). The absorption coefficient at a carefully chosen wavelength is thought by them to be a linear function of toluene internal vibrational energy, providing a direct monitor of energy transfer (much as IRF is used in the present study). Based upon the shape of the absorption decay curve (they cannot vary the excitation energy), Troe and co-workers have concluded that $\langle \Delta E(E) \rangle$ is constant, independent of E, for numerous collider gases. If this conclusion is correct, this may be another example of $\langle \Delta E(E) \rangle$ behavior. Since the excitation energy of the toluene is greater than the dissociation reaction critical energy (to give H + benzyl), it is also possible that this reactive system is exhibiting qualitatively different behavior than the nonreactive azulene system. This question should be addressed in future work: Is the energy-transfer process independent of whether the excitation energy is above or below a channel for unimolecular dissociation? Moreover, the free rotors in toluene and in substituted cycloheptatrienes may play an important role in the energy-transfer process, and we can ask whether different classes of vibrational modes exhibit different $\langle \Delta E(E) \rangle$ behavior. Direct experiments on energy transfer have the potential to answer such questions.

Discussion of collider behavior

Earlier workers found that the effectiveness of colliders tends to correlate with boiling point[1,48] and the number of atoms[1,2] of the collider. This correlation led directly to the idea of classes of colliders based on the number of transitional modes of the collision complex.[41] The present results tend to be in agreement with the earlier work, and it is convenient to discuss the results for various groups of gases. The following discussion refers to the data presented in Table V and in Fig. 7.

Monatomic cases

For this group of gases, there are only three transitional modes. The Lennard–Jones parameters are well known for these gases, and the relative collision frequencies are probably reliable to ±10%. The values for $\langle \Delta E(E) \rangle$ in Table V show reasonably consistent behavior. For excitation at 600 nm, the magnitude of $\langle \Delta E \rangle$ is a maximum for krypton; for 337 nm excitation, $\langle \Delta E \rangle$ magnitudes for argon and xenon are slightly larger than that for krypton, but the differences may not be signifi-

cant. All of the rare gases have $\langle \Delta E \rangle$ magnitudes less than 400 cm^{-1}, and the exponential model was used in the collisional master equation to simulate the data. Very good simulations were obtained for the values of β and γ shown in the table. For three of the gases, $\beta = 0$ and the significance (if any) of $\beta \neq 0$ for argon and krypton is not known.

Diatomic and linear triatomic gases

For this group of gases, there are five transitional modes. The effectiveness of energy transfer for H_2 and D_2 is about the same at 17 500 cm^{-1}, but there appears to be a small significant difference at 30 600 cm^{-1}. A comparison of He and D_2 shows that mass is not as important as rotational degrees of freedom in effecting energy transfer, since D_2 is considerably more effective than He.

A comparison of N_2, O_2, and CO shows great regularity of behavior. Considering uncertainties in collision frequencies and other sources of error, the results for these three gases are very similar. From these data there is no indication that spin-forbidden vibrational–electronic energy transfer plays any role in collisions involving O_2.

Carbon dioxide is considerably more effective than the diatomic gases. In light of the finding that V–V energy transfer takes place in this system,[16] it seems likely that the low-frequency bending mode may play an important role in the energy-transfer process. The frequency of this mode (667 cm^{-1}) is much lower than that of any of the diatomic gases studied.

For all of these gases, it was possible to obtain good fits using the expression for $\alpha(E)$ in the collisional master equation. Except for CO_2, the exponential model was chosen. For CO_2, with the magnitude of ΔE greater than 400 cm^{-1}, the reverse exponential model was chosen.

Nonlinear polyatomic gases

For this group of gases, there are six transitional modes, and one would expect them to be only slightly more effective colliders than the linear molecules. This is only partly true, however: methane is less effective than CO_2 in deactivating excited azulene. Possibly, this result is due to the absence of low-frequency methane modes.

The polar gases H_2O and NH_3 appear to be relatively efficient. This result may be partly due to the use of the Lennard–Jones potential for calculating collision frequency, rather than the Stockmayer potential. Azulene has a permanent dipole moment and it is possible that the collision frequency is underestimated, artificially increasing the magnitude of $\langle \Delta E \rangle$.

Taking the magnitudes of $\langle \Delta E \rangle$ for water and ammonia at face value, it is interesting that the low-frequency umbrella motion of NH_3 apparently plays no significant role in the energy-transfer process. When the collisional master equation was used in an attempt to simulate the data for these gases, it was found that the linear function assumed for $\alpha(E)$ does not produce self-consistent simulations of the data at 600 and 337 nm. If a good simulation is obtained for the rate constant corresponding to 600 nm, that for 337 nm is underestimated. Whether this effect is somehow related to the polarity of these molecules is not known.

A comparison of the values of $\langle \Delta E \rangle$ for methane, butane, and azulene shows that the functional behavior of $\langle \Delta E \rangle$ for CH_4 and butane are similar, but that for azulene is quite different. Butane is more effective than methane, possibly because of its many low-frequency vibrations and internal rotors, but azulene is more effective than either. The latter result is presumably due to the exact matching of vibrational frequencies. In earlier work,[49,50] we performed experiments with the time-dependent thermal-lensing technique and tentatively concluded that azulene may primarily undergo V–V energy transfer. Our conclusion (slightly strengthened in view of the newer values of $\langle \Delta E(E) \rangle$ for azulene and krypton in Table V) may be pertinent to the results found in the present work for deactivation of azulene. It is interesting, however, that $\langle \Delta E \rangle$ values for butane and azulene intersect at high energy in Fig. 7(a), predicting that butane may be a more effective collider than the parent gas under some conditions.

Although SF_6 possesses many low-frequency vibrations, it is less effective than butane and only a little more effective than CO_2 in deactivating azulene. The reason for this behavior is not known, but it may be dynamical, or it may be due to the role of "propensity rules" in governing transition probabilities.

In summary, energy-transfer parameters for excited azulene deactivation by 17 collider gases have been measured for two initial internal vibrational energies of the azulene. Two different analyses of the data were undertaken which employed different sets of reasonable assumptions and both resulted in values for $\langle \Delta E(E) \rangle$ which depend on energy. In ancillary experiments, V–V energy transfer was identified as a contributing process when CO_2 is used as a collider gas, and earlier time-dependent thermal-lensing experiments indicated that V–V energy transfer may dominate in azulene–azulene collisions. However, the evidence on the identity of the energy-transfer process is very limited and much work remains to be done. The important result that $\langle \Delta E(E) \rangle$ is a distinct function of energy will be useful for developing accurate models for energy transfer; some existing simple models show reasonable behavior in this regard. A wide variety of behavior is observed for $\langle \Delta E(E) \rangle$, and there is little theoretical basis for interpretation. Differences among gases are observed which cannot be simply explained, and one can only speculate about the causes involved. Thus, one cannot escape the conclusion that theory has lagged behind experiment in this field, and new theoretical efforts are needed.

ACKNOWLEDGMENTS

We are grateful for discussions with G. P. Smith, D. M. Golden, R. Patrick, B. S. Rabinovitch, H. Hippler, and J. Troe.

[1]D. C. Tardy and B. S. Rabinovitch, Chem. Rev. **77**, 369 (1977).
[2]M. Quack and J. Troe, Specialist Periodical Reports **2**, 175 (1977).
[3]G. P. Smith and J. R. Barker, Chem. Phys. Lett. **78**, 253 (1981).
[4]M. J. Rossi and J. R. Barker, Chem. Phys. Lett. **85**, 21 (1982).
[5]M. J. Rossi and J. R. Barker (unpublished results).
[6]H. Hippler, J. Troe, and H. J. Wendelken, Chem. Phys. Lett. **84**, 257 (1981).
[7]D. G. Gillespie and E. C. Lim, J. Chem. Phys. **68**, 4578 (1978).
[8]E. P. Ippen, C. V. Shank, and R. L. Woerner, Chem. Phys. Lett. **46**, 20 (1977).
[9]C. V. Shank, E. P. Ippen, O. T. Tesche, and R. L. Fork, Chem. Phys. Lett. **57**, 433 (1978).
[10]H. J. Kray and B. Nickel, Chem. Phys. **53**, 235 (1980).
[11]M. Comtet and H. O. Mette, Mol. Photochem. **2**, 63 (1970).
[12]H. Hippler reports ~ 1% quantum yield for isomerization observed with excimer laser photolysis at 248 nm (private communication).
[13]For a vibrational assignment, see R. S. Chao and R. K. Kahnna, Spectrochim. Acta Part A **33**, 53 (1977).
[14]G. Herzberg, *Infrared and Raman Spectra* (Van Nostrand, Princeton, 1945).
[15]J. F. Durana and J. D. McDonald, J. Chem. Phys. **64**, 2518 (1976).
[16]J. R. Barker, M. J. Rossi, and J. R. Pladziewicz, Chem. Phys. **90**, 99 (1982).
[17]J. R. Barker (unpublished results).
[18]P. R. Bevington, *Data Reduction and Error Analysis for the Physical Sciences* (McGraw-Hill, New York, 1969), p. 237.
[19]This figure supersedes that shown in Ref. 4, which suffered from a pressure-measurement error.
[20]More complex behavior is predicted in some systems (Ref. 21).
[21]J. E. Dove and S. Raynor, Paper 250, 28th Congress, International Union of Pure and Applied Chemistry, Vancouver, BC, 16–21 August 1981.
[22]For a review, see I. Oref and B. S. Rabinovitch, Acc. Chem. Res. **12**, 166 (1979).
[23]D. J. Nesbitt and S. R. Leone, Chem. Phys. Lett. **87**, 123 (1982).
[24]J. P. Maier, A. Seilmeier, and W. Kaiser, Chem. Phys. Lett. **70**, 591 (1980).
[25]R. C. Reid and T. K. Sherwood, *The Properties of Gases and Liquids* (McGraw–Hill, New York, 1966).
[26]L. Monchick and E. A. Mason, J. Chem. Phys. **35**, 1676 (1961).
[27]Reference 25, p. 400.
[28]J. Troe, J. Chem. Phys. **66**, 4758 (1977).
[29]Reference 25, p. 632.
[30]H. Hippler, suggested this approach (private communication).
[31]A. Bauder and H. H. Guenthard, Helv. Chim. Acta **45**, 1698 (1962).
[32]S. H. Fishtine, Z. Phys. Chem. **123**, 39 (1980).
[33]Reference 25, p. 38.
[34]J. Troe, J. Chem. Phys. **77**, 3485 (1982).
[35]J. R. Barker, Chem. Phys. (in press).
[36]For example, see K. D. King, T. T. Nguyen, and R. G. Gilbert, Chem. Phys. **61**, 221 (1981).
[37]R. K. Huddleston, G. T. Fuijmoto, and E. Weitz, J. Chem. Phys. **76**, 3839 (1982).
[38]H. Hippler, J. Troe, and H. J. Wendelken, Seventh International Symposium on Gas Kinetics, Göttingen, Germany, 23–27 August 1982; J. Chem. Phys. **76**, 5351 (1983); J. Chem. Phys. **78**, 6709 (1983).
[39]For a review of recent references, see J. T. Yardley, *Introduction to Molecular Energy Transfer* (Academic, New York, 1980).
[40]R. V. Serauskas and E. W. Schlag, J. Chem. Phys. **42**, 3009 (1965); **45**, 3706 (1966).
[41]Y. N. Lin and B. S. Rabinovitch, J. Phys. Chem. **74**, 3151 (1970).
[42]S. Nordholm, B. C. Freasier, and D. J. Jolly, Chem. Phys. **25**, 433 (1977).
[43]R. C. Bhattacharjee and W. Forst, Chem. Phys. **30**, 217 (1978).
[44]H. von Weyssenhoff and E. W. Schlag, J. Chem. Phys. **59**, 729 (1973).
[45]I. Oref and B. S. Rabinovitch, Chem. Phys. **26**, 385 (1977).
[46]H. W. Schranz and S. Nordholm, Int. J. Chem. Kinet. **13**, 1051 (1981).
[47]K. Y. Tang and C. S. Parmenter, J. Chem. Phys. (in press, and references cited therein).
[48]S. C. Chan, B. S. Rabinovitch, J. T. Bryant, L. D. Spicer, T. Fujimoto, Y. N. Lin, and S. P. Pavlou, J. Phys. Chem. **74**, 3160 (1970).
[49]J. R. Barker and T. Rothem, Chem. Phys. **68**, 331 (1982).
[50]P. L. Trevor, T. Rothem, and J. R. Barker, Chem. Phys. **68**, 341 (1982).